Nanoforest of Hydrothermally Grown Hierarchical ZnO Nanowires for a High Efficiency Dye-Sensitized Solar Cell

Seung Hwan Ko,*,[†] Daeho Lee,[§] Hyun Wook Kang,[†] Koo Hyun Nam,[†,‖] Joon Yeob Yeo,[†] Suk Joon Hong,[†] Costas P. Grigoropoulos,[§] and Hyung Jin Sung[†]

[†]Applied Nano Technology and Science Lab, Department of Mechanical Engineering, KAIST (Korea Advanced Institute of Science and Technology), 291 Daehak-ro, Yuseong-gu, 305-701, Korea

[§]Laser Thermal Laboratory, Department of Mechanical Engineering, University of California, Berkeley, California 94720-1740, United States

ABSTRACT: In this paper, in order to increase the power conversion efficiency we demonstrated the selective growth of "nanoforest" composed of high density, long branched "treelike" multigeneration hierarchical ZnO nanowire photoanodes. The overall light-conversion efficiency of the branched ZnO nanowire DSSCs was almost 5 times higher than the efficiency of DSSCs constructed by upstanding ZnO nanowires. The efficiency increase is due to greatly enhanced surface area for higher dye loading and light harvesting, and also due to reduced charge recombination by providing direct conduction pathways along the crystalline ZnO "nanotree" multi generation branches. We performed a parametric study to determine optimum hierarchical ZnO nanowire photoanodes through the combination of both length-wise growth and branched growth processes. The novel selective hierarchical growth approach represents a low cost, all solution processed hydrothermal method that yields complex hierarchical ZnO nanowire photoanodes by utilizing a simple engineering of seed particles and capping polymer.

KEYWORDS: Zinc oxide nanowire, dye-sensitized solar cell, nanoforest, hierarchical growth, branched structure
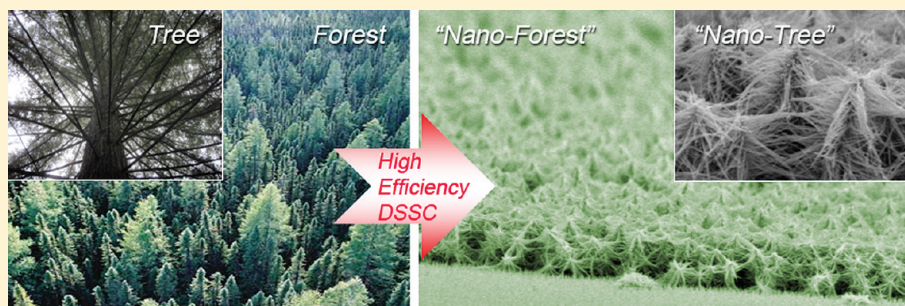
Dye-sensitized solar cells (DSSCs) based on oxide semiconductors and organic dyes or metallorganic-complex dye have recently emerged as the most promising candidate systems to achieve efficient solar-energy conversion since they are flexible, inexpensive, and easier to manufacture than silicon solar cells.[1−3] The DSSC is a photoelectrochemical system that incorporates a porous-structured wide-bandgap oxide semiconductor (TiO$_2$ or ZnO) film as the photosensitized anode offering increased surface area for dye molecule adsorption.[3] TiO$_2$ nanoparticles[3,4] or nanoporous structures[5,6] have been most extensively studied as a DSSC photoelectrode material. The respective record high conversion efficiency (11.2%) has persisted for nearly two decades.[7] Further increase in the conversion efficiency has been limited by energy loss due to recombination between electrons and either the oxidized dye molecules or electron-accepting species in the electrolyte during charge transport processes.[1,8−10] Such a recombination problem is more pronounced for TiO$_2$ nanocrystals due to the lack of a depletion layer on the TiO$_2$ nanocrystallite surface and becomes more serious when the photoelectrode film thickness increases.[1]

To understand and solve this issue, ZnO-based DSSC technology alternative to TiO$_2$ is considered as one of the most promising materials for solar cells. ZnO possesses energy band structure and physical properties similar to those of TiO$_2$, but its

electron mobility is higher by 2−3 orders of magnitude.[11] Therefore, ZnO is expected to exhibit faster electron transport with reduced recombination loss. Although the conversion efficiencies (0.4−5.8%) obtained for ZnO are much lower than the maximum reported 11% for TiO$_2$, ZnO is still thought of as the most promising alternative to TiO$_2$ due to its ease of crystallization and anisotropic growth.[1] Functional nanostructured photoelectrodes such as 1D nanostructures (nanowire,[1,2,12,13] nanotubes,[1,14] nanobelts,[15] nanosheets,[16,17] nanotips[18]) have been extensively studied and are expected to significantly improve the electron diffusion length in the photoelectrode films by providing a direct conduction pathway for the rapid collection of photogenerated electrons. Direct pathway along 1D crystalline nanostructures would diminish the possibility of charge recombination during interparticle percolation by replacing the conventional TiO$_2$ random polycrystalline nanoparticle network with ordered crystalline ZnO semiconductor nanowires (NWs). However, the insufficient surface area of simple 1D nanostructures constrains the energy conversion efficiency to relatively low levels (1.5% for ZnO NW DSSC[2]). Nanostructures

combining multiscale hierarchical configurations are particularly desirable for increased surface area and energy conversion efficiency. Suh et al.[19] and Baxter et al.[20] have presented a dendritic ZnO NW DSSC. They grew ZnO NWs by expensive chemical vapor deposition (CVD) and showed relatively low efficiency (0.5%) due to insufficient surface area. Jiang et al.[13] reported ZnO nanoflower photoanode and Cheng et al.[2] reported hierarchical ZnO NWs via a hydrothermal method. These hierarchical NWs were grown from seeds formed from $Zn(OAc)_2$ and still showed relatively low 1.5% efficiency, again due to insufficient surface area and also to the lack of uniformity of the secondary branches that were produced by the randomly distributed seed layer.

In this paper, we report that "nanoforest" of high density, long-branched "treelike" multigeneration hierarchical ZnO NW photoanodes can significantly increase the power conversion efficiency. The efficiency increase is due to substantially enhanced surface area enabling higher dye loading and light harvesting and also is due to reduced charge recombination by direct conduction along the crystalline ZnO nanotree multigeneration branches. This approach mimics branched plant structures with the objective to capture more sunlight. We performed parametric study to improve the efficiency of hierarchical ZnO NW photoanodes by combining length-wise growth (LG) and branched growth (BG).

Nanoforest of hierarchical ZnO NWs is grown by a hydrothermal growth approach modified from refs 12 and 21 as illustrated in Figure 1. Depending on the growth conditions, two types of growth modes are observed, lengthwise growth (LG) and branched growth (BG). LG can yield ZnO NWs of increased length by extending the growth at the tip of the backbone ZnO NW. On the other hand, BG produces highly branched ZnO NWs by multiple generation hierarchical growth. As shown in Figure 1a,b, first generation (backbone) ZnO NWs are grown from ZnO quantum dot seeds deposited on a substrate immersed in an aqueous precursor solution. ZnO quantum dots (3−4 nm) in ethanol are drop casted on a F−SnO₂ conductive glass (FTO) substrate to form uniform seeds for ZnO NW growth. NWs were grown by immersing the seeded substrate into aqueous solutions containing 25 mM zinc nitrate hydrate $[Zn(NO_3)_2 \cdot 6H_2O]$, 25 mM hexamethylenetetramine ($C_6H_{12}N_4$, HMTA) and 5−7 mM polyethylenimine (PEI) at 65−95 °C for 3−7 h.[12] After the reaction was complete, the grown ZnO NWs were thoroughly rinsed with Milli-Q water and dried in air to remove residual polymer. Longer ZnO NW can be produced by repeating the hydrothermal growth process in a fresh aqueous precursor solution per the LG mode sketched in Figure 1c. Dramatic change in the ZnO NW structure could occur by heating the first generation ZnO NW at 350 °C (10 min), adding seed NPs and subsequently applying hydrothermal growth. Instead of LG, highly BG of ZnO NW on the sidewalls of the first generation ZnO NW could be observed (Figure 1d). It should be noted that BG differs from LG only in that it involves the presence of a heating step and a seeding step before the regular hydrothermal growth. The combination of multiple LG and BG steps can be applied for more complex hierarchical ZnO NW structuring.

While a single hydrothermal reaction LG process can produce 2−8 μm long, vertically aligned ZnO NWs (130−200 nm diameter), multiple LG growth steps can grow 40−50 μm long ZnO NWs of high aspect ratio (>100). Figure 2a displays ZnO NW after 1,2,3 times LG steps. The length extension becomes smaller as the step order increases.

Vertically aligned long ZnO NWs grown by multiple LG steps can be used as the backbone of the hierarchical branched ZnO NW forest. High quality hierarchical branched ZnO NW forest
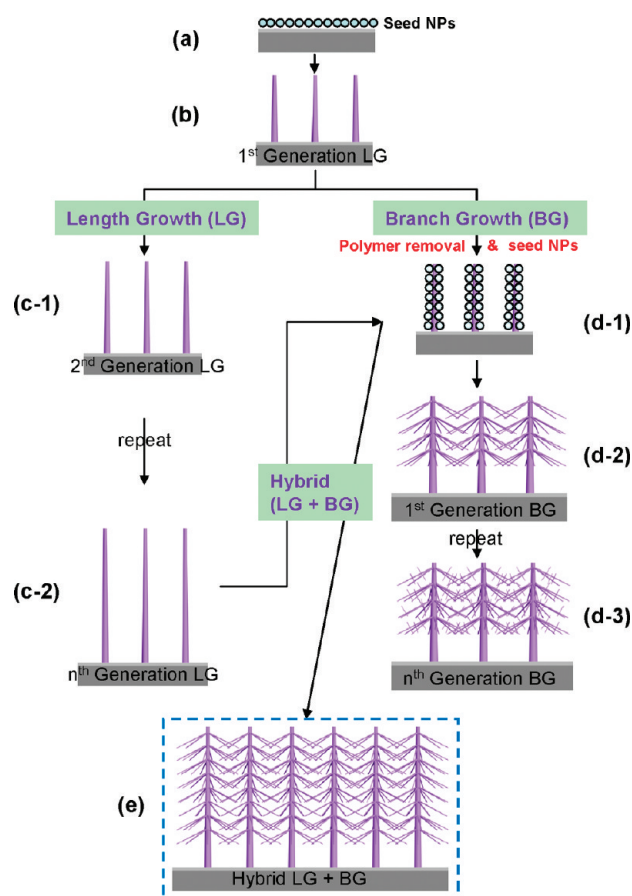

Figure 1. Two routes for hierarchical ZnO NW hydrothermal growth. Length growth (LG) (a-b-c), branched growth (BG) (a-b-d), and hybrid (a-b-c-d-e). Notice polymer removal and seed NPs for branched growth.

can be grown only after both (1) removal of polymer (HMTA, PEI) by heating the ZnO NW and (2) coating with seed NPs on the backbone ZnO NW surface. Figure 2b,c depicts the "seed effect" and Figure 2d,e shows the "polymer removal effect".

HMTA and PEI hinder only lateral growth but allow axial growth of the ZnO NWs in the solution, thus yielding high aspect ratio NWs.[12] The polymer can be removed by heating the ZnO NWs at 350 °C for 10 min. Branched growth (BG) that had been previously suppressed by HMTA and PEI during regular LG could be induced once the polymer was removed from the backbone NW, as shown in Figure 2b. In addition to random and sparsely branched NW growth on the side walls, the diameter of first generation backbone ZnO NW also increased (~1 μm) due to lateral growth after the removal of the HMTA and PEI polymer layer. After the polymer removal, seed NP coating on the first generation backbone NWs could induce growth of densely packed higher order generation BG while suppressing the diameter increase of the first generation backbone NW (Figure 2c).

ZnO seed NP coating on the backbone ZnO NW without polymer removal could grow just sparsely branched ZnO NW (Figure 2d). In contrast, high quality hierarchical branched ZnO NW forest could be achieved by coating the backbone ZnO NW with ZnO seed NP after polymer removal (Figure 2e). ZnO NW growth from the seed NP on HMTA and PEI polymer may be less favorable than on the ZnO NW surface without polymer.
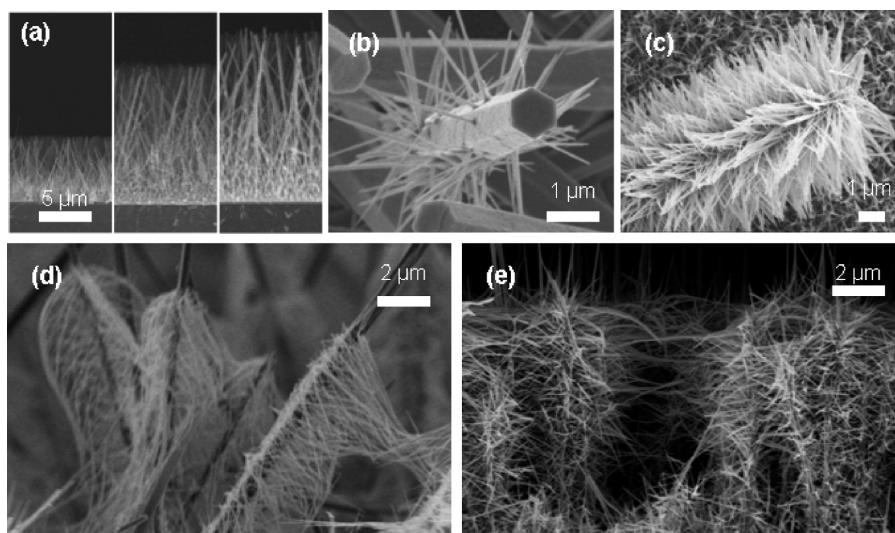
Figure 2. SEM pictures of ZnO NWs. (a) Length growth (1,2,3 times growth). Seed effect: first generation branched growth (b) without seeds and (c) with seeds after polymer removal. Polymer removal effect: first generation branched growth (d) without polymer removal and (e) with polymer removal after seed NP deposition. Polymers on ZnO NW are removed after 350 °C heating for 10 min.
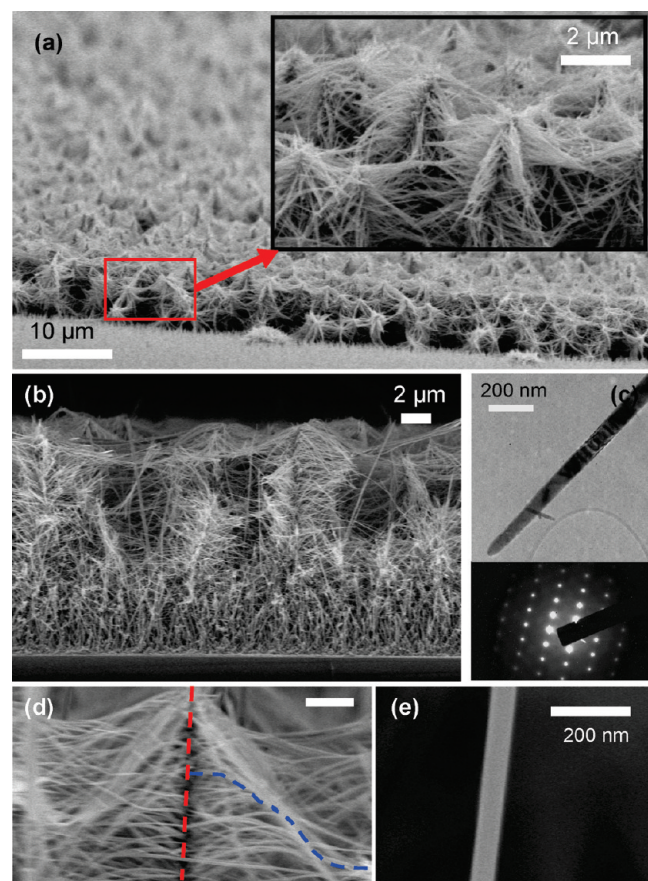

Figure 3. SEM pictures of ZnO NW nanoforest: (a) tilted view, (b) cross section view, (d) magnified view of backbone (red dotted line) and first generation branches (blue dotted line), and (e) magnified view of a branch. (c) TEM picture and selected area electron diffraction pattern of a ZnO NW.

This signifies that both polymer removal and seed layer addition are important for realizing high density hierarchical branched ZnO NW forest growth.

Nanoforest of the hierarchical branched ZnO NW could be easily grown on a large area (Figure 3a) by a low cost, all solution processed hydrothermal method. The quality of the ZnO NWs has been characterized by scanning electron microscope (SEM) and transmission electron microscope (TEM). The tilted view (Figure 3a) and cross sectional images (Figure 3b,d) of the ZnO NWs suggest that the hierarchically branched ZnO NW (indicated by the blue dotted lines in Figure 3d) grow perpendicular to the vertically oriented first generation backbone ZnO NWs surface (indicated by the red dotted lines in Figure 3d) surface. The length of branched ZnO NWs was $2-10$ μm upon a single growth step and their diameter (Figure 3e) usually in the range of $30-50$ nm, hence always much smaller than the diameter of first generation backbone ZnO NW ($130-200$ nm). This is attributed to the fact that branched ZnO NWs extended from the faces of the hexagonal backbone ZnO NWs. Both backbone ZnO NWs and branched ZnO NWs have hexagonal cross sections and grow along the c axis of the wurtzite crystal. TEM characterization of individual NWs indicates that they are single-crystalline and grow in the [0001] direction (Figure 3c, TEM picture; inset: selected area electron diffraction (SAED) pattern). While the branched growth NW and the backbone ZnO NWs have monolithically single crystalline relationship for CVD grown comblike ZnO nanostructure,[22,23] the hydrothermally grown secondary branched ZnO NW did not originate from the backbone NW but from the ZnO seed nanoparticles in the c axis direction of single crystal wurtzite structure.[2]

High-efficiency DSSCs could be demonstrated from the densely z+s (Hartford Inc.). Figure 4a shows the schematic picture of the DSSC and the SEM magnified picture of the ZnO NW nanoforest. ZnO NWs were rinsed with DI water and baked in air at 350 °C for 30 min to remove any residual organics and optimize solar cell performance.[12] Then ZnO NWs were sensitized in a solution of 0.5 mM cisbis(isothiocyanato)bis(2,2′-bipyridyl-4,4′-dicarboxylato)-ruthenium(II) bis-tetrabutylammonium (N719, Solaronix) in dry ethanol for 5 h and then sandwiched together and bonded with platinum catalyst coated FTO counter electrodes separated by 40 μm thick hot melt foil spacer. The electrolyte solution (0.1 M LiI, 0.5 M 1,2-dimethyl-3-propylimidazolium
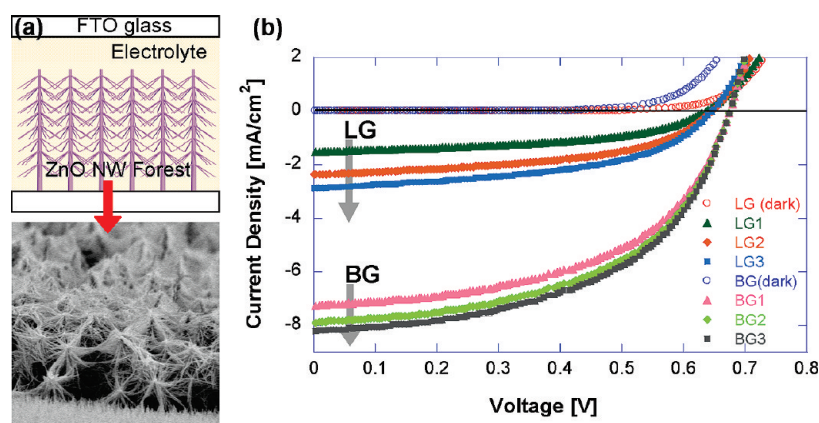
Figure 4. (a) Schematic structure and (b) $J-V$ curve of dye-sensitized solar cell with "nano-forest" ZnO NW.

Table 1. Characteristics of "Nanoforest" DSSC Solar Cells in Figure 4b

Symbol	Backbone NW length [μm]	Branching times	Configuration	Efficiency [%]	J_{sc} [mA/cm²]	V_{oc} [V]	FF
LG1	7			0.45	1.52	0.636	0.480
LG2	13	0		0.71	2.37	0.64	0.486
LG3	18			0.85	2.87	0.645	0.484
BG1	7	1		2.22	7.43	0.681	0.522
BG2	13	1		2.51	8.44	0.683	0.531
BG3		2		2.63	8.78	0.680	0.530

iodide, 0.03 M I_2, and 0.5 M tert-butylpyridine in acetonitrile)[2] was introduced via capillary action into the gap formed by the two electrodes. The current density versus voltage ($J-V$) characteristics of the cells were measured under AM1.5G 100 mW/cm² illumination from a solar simulator (Newport) immediately after cell assembly.

Figure 4b shows the $J-V$ characteristics for solar cells with both BG and LG ZnO nanostructures and the DSSC characteristics are summarized in Table 1. $J-V$ curves for upstanding ZnO NW with various lengths (LG1, 7 μm; LG2, 13 μm; LG3, 16 μm) are presented in Figure 4b. The short circuit current density (J_{SC}) and the overall light conversion efficiency increased as the length of the LG ZnO NW increased (LG1, 0.45%; LG2, 0.7%; LG3, 0.85%) due to effective surface area increase. One-time branched growth on LG1 (7 μm) and LG2 (13 μm) yielded BG1 (from LG1) and BG2 (from LG2) and two-time branched growth produced BG3 (from LG2). By implementing additional NW generations, the short circuit current density (J_{SC}) and overall light conversion efficiency could be significantly increased for high density hierarchical branched ZnO NW nanoforest. The respective enhancement was in the range of by 350−500% for the same

backbone NW length (LG1, 0.45% to BG2, 2.22%; LG2, 0.71% to BG2, 2.51%). This is much higher than the reported values[2,7] for hierarchical ZnO NW DSSC and related to the substantial effective area increase by BG. The efficiency increase can be explained by considering a combination of several effects. First, the enhanced photon absorption associated with the augmented surface area results in increased dye loading and correspondingly to large J_{SC} increase. LG can grow only upstanding NWs by adding length to the first generation backbone NW. However, BG can grow multibranched NWs from just a single first generation backbone NW, thus surface area can be increased dramatically. The measured NW number density for upstanding LG NW (10^9 /cm²) could be increased by 1−2 orders of magnitude (10^{10-11} /cm²) by branched NW growth. Second, a dense network of crystalline ZnO NWs can increase the electron diffusion length and electron collection because the NW morphology provides more direct conduction paths for electron transport from the point of injection to the collection electrode. Third, randomly branched NWs promote enhanced light-harvesting (light-dye interaction) without sacrificing efficient electron transport. In contrast, upstanding NWs are not favorable for light harvesting because photons

could possibly travel between the vertical NWs without being absorbed by the dye.[13] Furthermore, branched NWs can increase light-harvesting efficiency by scattering enhancement and trapping.[1] The fill factor (FF) values for ZnO DSSCs are generally lower than those obtained using TiO_2 nanoparticles (0.6−0.7). This is attributed to recombination between photoexcited carriers in the photoanodes and tri-iodide ions in the electrolyte. The FF may be enhanced by implementing dc or radio frequency magnetron sputtering and atomic layer deposition.[2]

In summary, we have demonstrated nanoforest of high density, long branched treelike multigeneration hierarchical crystalline ZnO NW photoanodes via a simple selective hierarchical growth sequence and could significantly improve the DSSC power conversion efficiency. The short-circuit current density and overall light-conversion efficiency of the branched ZnO NW DSSCs were almost 5 times higher than the efficiency of upstanding ZnO NWs. The efficiency increase is due to greatly augmented surface area enabling higher dye loading and light harvesting, as well as to reduced charge recombination through direct conduction along the crystalline ZnO nanotree multigeneration branches. We performed a parametric study to define hierarchical ZnO NW photoanodes consisting of various generation NWs through the combination of length-wise and branched growth. Complex, hierarchical ZnO NW photo-anodes can be fabricated via this low cost, all solution processed hydrothermal method incorporating seed particle deposition steps and utilization of capping polymers. Since the process takes place at low temperatures, it carries substantial potential for further developing DSSCs on low-cost, large-area flexible polymer substrates. Low-temperature laser annealing of metal oxide[24] and metal nanomaterial[25−28] can be directly combined to realize flexible solar cells.

■ AUTHOR INFORMATION

Corresponding Author
*E-mail: maxko@kaist.ac.kr.

Present Addresses
‖Current address: Institute for the Early Universe and Research Center of MEMS Space Telescope, Ewha Womans University, Seoul, 120-750, Korea.

■ ACKNOWLEDGMENT

■ REFERENCES

(1) Zhang, Q.; Dandeneau, C. S.; Zhou, X.; Cao, G. ZnO nanostructures for Dye-sensitized Solar Cells. *Adv. Mater.* **2009**, *21*, 1–22.

(2) Cheng, H.; Chiu, W.; Lee, C.; Tsai, S.; Hsieh, W. Formation of Branched ZnO Nanowires from Solvothermal Method and Dye-Sensitized Solar Cells Applications. *J. Phys. Chem. C.* **2008**, *112*, 16359–16364.

(3) Oregan, B.; Gratzel, M. A Low Cost, High-Efficiency Solar Cell Based on Dye-sensitized Colloidal TiO_2 Films. *Nature* **1991**, *353*, 737.

(4) Ma, T.; Akiyama, M.; Abe, E.; Imai, I. High-Efficiency Dye-Sensitized Solar Cell Based on a Nitrogen-Doped Nanostructured Titania Electrode. *Nano Lett.* **2005**, *5*, 2543.

(5) Crossland, E. J. W.; Kamperman, M.; Nedelcu, M.; Ducati, C.; Wiesner, U.; Smilgies, D.-M.; Toombes, G. E. S.; Hillmyer, M. A.; Ludwigs, S.; Steiner, U.; Snaith, H. J. A Bicontinuous Double Gyroid Hybrid Solar Cell. *Nano Lett.* **2009**, *9*, 2807.

(6) Guldin, S.; Hüttner, S.; Kolle, M.; Welland, M. E.; Mller-Buschbaum, P.; Friend, R. H.; Steiner, U.; Tétreault, N. Dye-Sensitized Solar Cell Based on a Three-Dimensional Photonic Crystal. *Nano Lett.* **2010**, *10*, 2303.

(7) Yang, Z.; Xu, T.; Ito, Y.; Welp, U.; Kwok, W. K. Enhanced Electron Transport in Dye-Sensitized Solar Cells Using Short ZnO Nanotips on A Rough Metal Anode. *J. Phys. Chem. C* **2009**, *113*, 20521–20526.

(8) Nissfolk, J.; Fredin, K.; Hagfeldt, A.; Boschloo, G. Recombination and Transport Processes in Dye-Sensitized Solar Cells Investigated under Working Conditions. *J. Phys. Chem. B* **2006**, *110*, 17715.

(9) Gratzel, M. Solar Energy Conversion by Dye-Sensitized Photovoltaic Cells. *Inorg. Chem.* **2005**, *44*, 6841.

(10) Gratzel, M. Conversion of sunlight to electric power by nanocrystalline dye-sensitized solar cells. *J. Photochem. Photobiol., A* **2004**, *164*, 3.

(11) Pan, H.; Misra, N.; Ko, S. H.; Grigoropoulos, C. P.; Miller, N.; Haller, E. E.; Dubon, O. Melt-mediated coalescence of solution-deposited ZnO nanoparticles by excimer laser annealing for thin-film transistor fabrication. *Appl. Phys. A* **2009**, *94*, 111.

(12) Law, M.; Greene, L. E.; Johnson, J. C.; Saykally, R.; Yang, P. Nanowire Dye-sensitized Solar Cells. *Nat. Mater.* **2005**, *4*, 455.

(13) Jiang, C. Y.; Sun, X. W.; Lo, G. Q.; Kwong, D. L.; Wang, J. X. Improved dye-sensitized solar-cells with a ZnO-nanoflower photoanode. *Appl. Phys. Lett.* **2007**, *90*, No. 263501.

(14) Martinson, A. B. F.; Elam, J. W.; Hupp, J. T.; Pellin, M. J. ZnO Nanotube Based Dye-Sensitized. Solar Cells. *Nano Lett.* **2007**, *7*, 2183–2187.

(15) Wang, X. D.; Ding, Y.; Summers, C. J.; Wang, Z. L. Large-Scale Synthesis of Six-Nanometer-Wide ZnO Nanobelts. *J. Phys. Chem. B* **2004**, *108*, 8773.

(16) Kar, S.; Dev, A.; Chaudhuri, S. Simple Solvothermal Route to Synthesize ZnO Nanosheets, Nanonails, and Well-Aligned Nanorod Arrays. *J. Phys. Chem. B* **2006**, *110*, 17848.

(17) Fu, M.; Zhou, J.; Xiao, Q. F.; Li, B.; Zong, R. L.; Chen, W.; Zhang, J. ZnO nanosheets with ordered pore periodicity via colloidal crystal template assisted electrochemical deposition. *Adv. Mater.* **2006**, *18*, 1001.

(18) Wang, Z. L. Zinc oxide nanostructures: growth, properties and applications. *J. Phys.: Condens. Matter* **2004**, *16*, R829.

(19) Suh, D. I.; Lee, S. Y.; Kim, T. H.; Chun, J. M.; Suh, E. K.; Yang, O. B.; Lee, S. K. The fabrication and characterization of dye-sensitized solar cells with a branched structure of ZnO nanowires. *Chem. Phys. Lett.* **2007**, *442*, 348.

(20) Baxter, J. B.; Aydil, E. S. Dye-sensitized solar cells based on semiconductor morphologies with ZnO nanowires. *Sol. Energy Mater. Sol. Cells* **2006**, *90*, 607.

(21) Ko, S. H.; Park, I.; Pan, H.; Misra, N.; Rogers, M. S.; Grigoropoulos, C. P.; Pisano, A. P. ZnO nanowire network transistor fabrication on a polymer substrate by low-temperature, all-inorganic nanoparticle solution process. *Appl. Phys. Lett.* **2008**, *92*, No. 154102.

(22) Wang, Z. L.; Kong, X. Y.; Zuo, J. M. Induced growth of asymmetric nanocantilever arrays on polar surfaces. *Phys. Rev. Lett.* **2003**, *91*, No. 185502.

(23) Yan, H.; He, R.; Johnson, J.; Law, M.; Saykally, R.; Yang, P. Dendrite Nanowire UV Laser Array. *J. Am. Chem. Soc.* **2003**, *125*, 4728.

(24) Pan, H.; Ko, S. H.; Misra, N.; Grigoropoulos, C. P.; Pisano, A. P. Laser annealed composite titanium dioxide electrodes for dye-sensitized solar cells on glass and plastics. *Appl. Phys. Lett.* **2009**, *94*, No. 071117.

(25) Ko, S. H.; Pan, H.; Grigoropoulos, C. P.; Luscombe, C. K.; Fréchet, J. M. J.; Poulikakos, D. All-inkjet-printed flexible electronics fabrication on a polymer substrate by low-temperature high-resolution selective laser sintering of metal nanoparticles. *Nanotechnology* **2007**, *18*, 345202.

(26) Ko, S. H.; Park, I.; Pan, H.; Grigoropoulos, C. P.; Pisano, A. P.; Luscombe, C. K.; Fréchet, J. M. J. Direct Nanoimprinting of Metal Nanoparticles for Nanoscale Electronics Fabrication. *Nano Lett.* **2007**, *7*, 1869.

(27) Ko, S. H.; Pan, H.; Hwang, D. H.; Chung, J.; Ryu, S.; Grigoropoulos, C. P.; Paulikakos, D. High resolution selective multilayer laser processing by nanosecond laser ablation of metal nanoparticle films. *J. Appl. Phys.* **2007**, *102*, No. 093102.

(28) Ko, S. H.; Pan, H.; Grigoropoulos, C. P.; Fréchet, J. M. J.; Luscombe, C. K.; Poulikakos, D. Lithography-free high-resolution organic transistor arrays on polymer substrate by low energy selective laser ablation of inkjet-printed nanoparticle film. *Appl. Phys. A* **2008**, *92*, 579.